Research article

MRC

Received: 4 December 2013 Revised: 28 January 2014 Accepted: 17 February 2014 Published online in Wiley Online Library

(wileyonlinelibrary.com) DOI 10.1002/mrc.4058

Pyridylalkylamine ligands and their palladium complexes: structure and reactivity revisited by NMR

Alexandre Requet,[a] Olivier Colin,[a] Flavien Bourdreux,[a] Salim M. Salim,[a] Sylvain Marque,[a] Christine Thomassigny,[a] Christine Greck,[a] Jonathan Farjon[b]** and Damien Prim[a]*

Pyridylmethylamines or pma are versatile platforms for different catalytic transformations. Five pma-ligands and their respective Pd complexes have been studied by liquid state NMR. By comparing ^{1}H, ^{13}C and ^{15}N chemical shifts for each pma/pma–Pd couple, a general trend for the metallacycle atoms concerns variations of the electronic distribution at the pendant arm, especially at the nitrogen atom of the ligand. Moreover, the increase of the chemical shift of the pendant arm nitrogen atom from primary to tertiary amine is also related to the increase of crowding within the complex. This statement is in good agreement with X-ray data collected for several complexes. Catalytic results for the Suzuki–Miyaura reaction involving the pma–Pd complexes showed within this series that a sterically crowded and electron-rich ligand in the metallacycle was essential to reach the coupling product with a good selectivity. In this context, NMR study of chemical shifts of all active nuclei especially in the metallacycle could give a trend of reactivity in the studied family of pma–Pd complexes. Copyright © 2014 John Wiley & Sons, Ltd.

Keywords: NMR; ^{15}N; ^{1}H; ^{13}C; pyridylmethylamine; *N*-heterocyclic benzhydrylamines; *N,N*-bidentate ligands; palladium

Introduction

The installation of a pendant methylamine arm at pyridine rings generates an ideal 1,2-*N,N*-bidentate ligand and confers to the so-called pyridylmethylamine (pma) scaffold interesting complexation properties. Such motif can be encountered in numerous bioinspired Cu-, Fe-, Re-, or Zn-based coordination compounds.[1] The combination of pma and transition metals revealed especially valuable as catalytic systems in synthetic transformations such as various oxidative processes,[2] cycloaddition of dienes,[3] Henry reactions,[4] and Friedel–Crafts alkylations[5–7] driving the interest of the scientific community for new and robust pma-based catalytic systems. We recently contributed to this area and reported on the synthesis, complexation, and catalysis using pma–Pd[8–11] and pma–Cu combinations.[8] In the context of Suzuki–Miyaura C–C bond formation using pma–Pd catalytic systems, it has been shown that the substitution at the benzylic position of the pendant arm was of major importance to obtain high conversions (Fig. 1). These first sets of results were completed by solid state X-ray data arising from several pma–Pd complexes, which evidenced a close overall geometry and a similar spatial arrangement of substituents in all complexes.

Our objectives are to gain further information and complementary structure–reactivity data in the context of catalytic activity of the pma family. With these aims, liquid state NMR techniques were implemented to fully probe various pyridylalkylamine ligands and their respective Pd complexes. In this context, heteronuclear ^{1}H–X (X: ^{15}N, ^{13}C) NMR correlations through well-known HMBC[12] experiments revealed a useful and crucial tool to estimate the contribution of surrounding substituents of the nitrogen atom in solution where the reaction took place. Results in solution have been compared with solid state data, evidencing a clear impact of the substitution pattern around the pendant arm nitrogen atom including the class of the amine on characteristic metal-N bonds in Pd complexes. Within the pma family, attempts to determine whether a tertiary-based or a secondary amine-based catalyst and the nature of substituents would be beneficial to catalytic properties were realized in biphenyl and binaphthyl model series. In the following, the synthesis of different ligands will be described.

Results and Discussion

Synthesis of ligands and complexes

We first focused on the preparation of five pma ligands and their corresponding complexes (Fig. 2). Ligands **1–3** were obtained in high yields from pyridine-2-carbonitrile and phenylmagnesium chloride, pyridine-2-carboxaldehyde and benzylamine or methylbenzylamine, respectively (Scheme 1).

* *Correspondence to: Damien Prim, Université de Versailles Saint-Quentin-en-Yvelines, Institut Lavoisier de Versailles UMR CNRS 8180, 45, avenue des Etats-Unis, 78035 Versailles, France. E-mail: damien.prim@uvsq.fr*

** *Correspondence to: Jonathan Farjon, Equipe RMN en milieu Orienté, Institut de Chimie Moléculaire et des Matériaux d'Orsay (ICMMO), UMR CNRS 8182, bât. 410, Université Paris-Sud, 91405 Orsay, France. E-mail: jonathan.farjon@u-psud.fr*

a *Université de Versailles Saint-Quentin-en-Yvelines, Institut Lavoisier de Versailles, UMR CNRS 8180, 45, avenue des Etats-Unis, 78035 Versailles, France*

b *Equipe RMN en milieu Orienté, Institut de Chimie Moléculaire et des Matériaux d'Orsay (ICMMO), UMR CNRS 8182, bât. 410, Université Paris-Sud, 91405 Orsay, France*

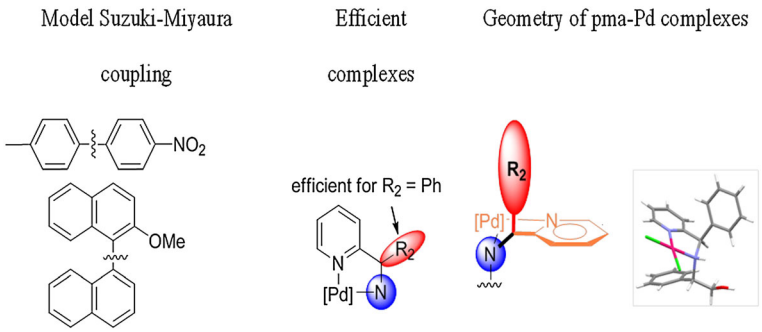

Figure 1. First sets of characteristic data in the pma family.

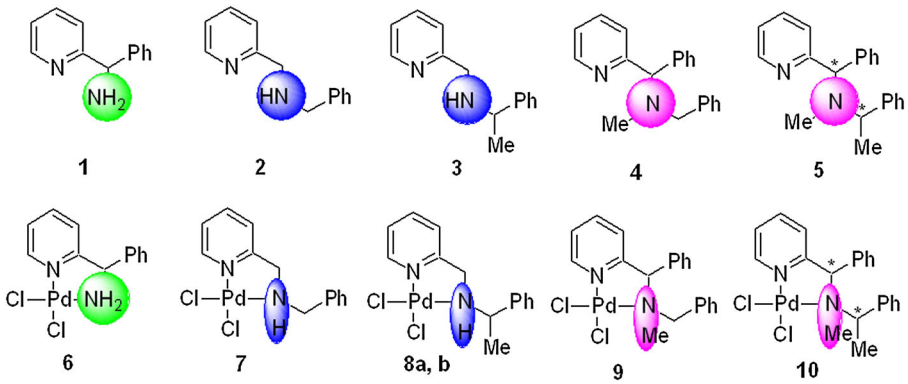

Figure 2. Series of pma ligands **1–5** and complexes **6–10**.

Ligands **4** and **5** were prepared through methylation starting of already reported pma derivatives.[7] The pendant arm within this series consists of one primary, two secondary, and two tertiary amines. The primary amine **1** displays a phenyl group at the benzylic position. Secondary amines in one part and tertiary amines in the other part differ each other by the increasing steric hindrance of the additional substituent (**2** vs **3** and **4** vs **5**). At least, we focused on **5**/**10** as a new ligand-complex couple that combines both a phenyl group at the benzylic position and two additional methyl groups. Ligands **1–5** were then reacted with Na_2PdCl_4 in freshly distilled MeOH to afford the complexes **6–10**. As already observed for ligands bearing nonracemic groups, the presence of stereodefined carbon centers in ligand **3**[8] controls the central chirality on the nitrogen atom and induces the formation of the two diastereomers **8a** and **8b** during the complexation process. Although they could not be separated, ^{1}H NMR spectra display two characteristic sets of signals (Table 1 SI). It is worth noting that the increase of steric crowding at the pendant arm nitrogen atom allowed complexation without noticeable impacts on yield, complex **10** being isolated in a fair 88% yield.

NMR is a well-known technique that will help to rationalize structure, electronic distribution, and steric effects with reactivity of the complexes under study.

^{1}H, ^{13}C and ^{15}N NMR studies for a full characterization of ligands 1–5 and complexes 6–10

Numbering system for all ligands and complexes is shown in Fig. 3.

By the way of chemical shifts, the effect of the metal chelation has been investigated by comparing the chemical shifts of the ligand and the complex for each active atom i through $\Delta_i = \delta_i$ (complex)-δ_i(ligand).[12] Tables 1–4 SI gather chemical shifts but also Δ_i for characteristic protons and carbons. Further data could arise from analysis of ^{15}N chemical shifts. However, classical 1D ^{15}N NMR analysis appears time consuming because of low isotopic natural abundance (0.36%) and long T_1 relaxation times. Thus, evaluation of coordination and analysis of chemical shift variation between complex and ligand have been obtained through more sensitive ^{1}H-detected heteronuclear ^{1}H–^{15}N HMBC[13] correlations (Fig. 1 SI and Table 1).

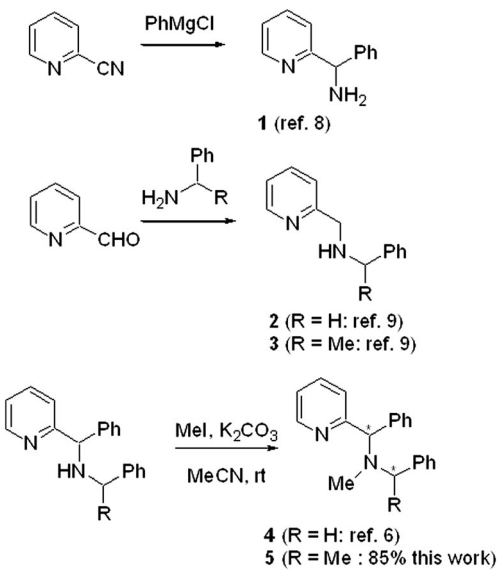

Scheme 1. Preparation of ligands **1–5**.

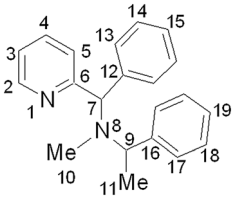

Figure 3. Numbering system adopted in the pma family.

Careful examination of NMR spectra and calculated Δδ warrants some additional comments. In a general manner whatever the nuclei, Δ_i is not zero, meaning that the Pd is chelated to the ligand and that all nuclei (i.e. ^{1}H, ^{13}C, and ^{15}N) are spies feeling the complexation. As expected, almost all protons undergo the influence of the presence of the metal in the complexes **6–10**. Pyridinic protons (H2–5) show Δδ averaged ranging from 0.03 to 0.60 ppm. Probe protons, namely H7 and H9 exhibit characteristic-enhanced Δδ values from **1**/**6** to **5**/**10** couples. First, H7 are privileged spectator *vis-à-vis* the complexation to the palladium atom being localized into the metallacycle. Second, the increase of the substitution at the pendant arm nitrogen atom impacts Δδ. A clear shielding from a ligand to another one is observed and induces an increasing of the Δδ from primary (Δδ = 0.35) for couple **1**/**6**, to tertiary amine (Δδ = 0.81) for the couple **4**/**9**. A similar trend can be observed for H9, albeit in a lesser extent (secondary for **3**/**8a**, **8b** vs tertiary for **4**/**9**: Δδ ≈ 0.5 vs Δδ > 0.6) (Table 1 SI). Moreover, the chelation of the Pd affects aromatic nuclei. Deshieldings for benzylic ^{1}H are in the same range for complexes **7** and **8a**/**8b**. The more impacted protons in these two complexes are H7 and H9, being localized in α position to N8. However, for the complexes **9** and **10**, benzylic protons H17, H18, and H19 have a highest deshielding than the complexes **7**, **8a**, and **8b**. This is plausibly due to the fact that electrons are more dispersed in the complexes **9** and **10** due to a supplementary Ph group. In the case of the phenyl moiety, H14 and H15 have almost the same deshielding in the complexes **6** and **9** (Table 2 SI).

Effect of complexation can also be observed at carbon atoms. Indeed, if C3–C6 are characterized by a Δaveraged ranging from 1.2 to 4.2 ppm, C2 is poorly affected by the presence of the metal (Δaveraged = 0.2–0.5 ppm). In contrast, C7, C9, and C10 undergo major impact of the presence of the Pd atom depending on substituents of the amine atom. Δδ for C7 that is embedded into the metallacycle decreases from the primary to the tertiary amine from 5.4 to 3.7 ppm from ligand/complex couples **1**/**6** to **4**/**9**. In addition, the largest Δδ of 14.5 and 17.3 ppm is observed between structures **5** and **10** characterized by the presence of a tertiary amine (Table 3 SI).

We next turned our attention to the impact of the complexation on both nitrogen atoms being the most affected nuclei due to their close contact to the metal. Table 1 gathers ^{15}N chemical shifts and Fig. 1 SI shows examples of heteronuclear ^{1}H-^{15}N correlations on primary, secondary and tertiary ligand-complex couples. Overlapping of both ligand and complex heteronuclear ^{1}H-^{15}N correlations clearly evidenced influence of complexation over ^{15}N chemical shifts. For ligands **1** to **5**, δN1 changes in a range of 1 to 4 ppm showing that this site is only poorly affected by substituents at the pendant arm. In contrast, δN8 exhibit a large shielding up to +13 ppm (between ligands **1** and **3**) most plausibly arising from the presence of increasing donating groups from a primary to a tertiary amine. It is worth noting that the comparison of chemical shifts of the pyridinic nitrogen atom N1 in the ligand-complex couples shows a large deshielding of restraint range from −88 to −93 ppm. In deep contrast, the pendant arm nitrogen atom N8 appears less affected by the presence of the palladium atom. Indeed, Δδ for N8: ΔN8 ranged from -20 to +8 ppm. This is due to the fact that only N1 is involved in the pyridine ring and π-backbonding allows stabilizing the Pd-N1 bond. Moreover, Δδ for N1 are almost insensitive to the pendant arm substitution, it changes up to 5 ppm from **1**/**6** to **5**/**10** couples.

This trend results from contributions of two main factors. First, the presence of additional electron donating groups that shield N8. In the following, we will detail the contribution of each ornamental moiety of the pending arm of the ligand. ΔN8 increase up to 8 ppm, meaning that all added groups enrich the N8 and therefore directly impacted the Pd–N8 bond strength. Some additional trends and effects of each substituents can be given within these series of couples: (i) from 1 to 8 ppm shielding effect of benzylic methyl groups on chemical shifts (Table 1, compare couples **2**/**7** vs **3**/**8a**/**8b** and **4**/**9** vs **5**/**10**), (ii) combined effect of benzyl and *N*-methyl groups leads to large shielding up to 20.6 ppm (Table 1, compare couples **1**/**6** vs **4**/**9**), (iii) combined effect of phenyl and *N*-methyl groups also shows positive shielding of 14.1 ppm (Table 1, compare **2**/**7** vs **4**/**9**), and (iv) the presence of *N*-methyl group results in shielding of 6 ppm (Table 1, compare **4**/**9** vs **2**/**7** and vs **1**/**6**). Consequently, the Ph leads to a shielding of 8 ppm and the benzyl group to a shielding of 14 ppm. The second effect explaining the increase of the ΔN8 is the strong enhancement of the steric crowding from **1**/**6** to **5**/**10** at the pendant arm nitrogen atom that plausibly concomitantly increases the Pd–N8 strength.

Solid state study confirmed the liquid state NMR analytical picture.

Within this series, five crystal structures of pma–Pd complexes,[14] have already been reported by us, evidencing that all complexes adopt similar 3D geometry whatever the nature of substituents at the pendant arm and of amine class (Table 2).

Although secondary and tertiary amine-based complexes present similar molecular arrangements, noticeable differences exist between both types of complexes. As evidenced in Table 3, length of Pd–N1 bonds are close (2.020–2.025 Angströms) regardless of the amine class within this series. In deep contrast, Pd–N8 bonds are much longer for tertiary amines by comparison with

Table 1. ^{15}N chemical shifts for free ligands and complexes, Δ = δN (complex)-δN(ligand) is given between brackets

Ligand/complex	N1[a]	N8[a]
1	−67	−342
6	−155 (−88)	−362 (−20)
2	−65	−342
7	−154 (−89)	−356 (−14)
4	−63	−332
9	−156 (−93)	−332 (0)
3	−66	−329
8a/8b	−155/−153 (−89/−88)	−342/−342 (−13/−13)
5	−63	−330
10	−156 (−93)	−322 (+8)

[a]Negative ^{15}N chemical shifts are referred to external pure CH_3NO_2 (its $\delta_{15N} = 0$ ppm). The ^{1}H–^{15}N HMBC has been used for detecting the ^{15}N chemical shift of NO_2 due to the evolution of $^{2}J_{H-N}$ coupling.

Table 2. X-ray details and selected crystallographic data

Spatial arrangement for pma-based complex	Complex	CCDC (Ref.)	Pd–N1(Angströms)	Pd–N8(Angströms)
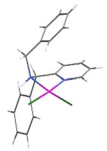	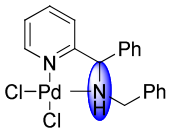	677 262 (6)	2.021	2.031
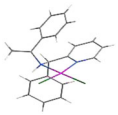	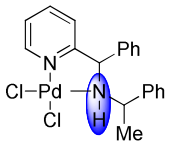	812 300 (8)	2.020	2.043
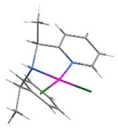	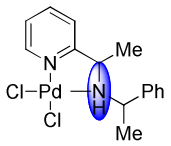	812 301 (8)	2.025	2.038
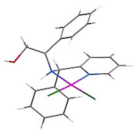	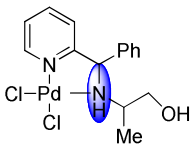	812 302 (8)	2.020	2.043
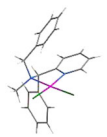	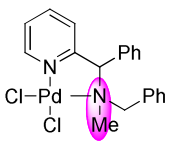 **9**	677 264 (6)	2.020	2.083

secondary amines (2.083 Angströms vs 2.031–2.043 Angströms) in full agreement with an increase of steric crowding at the tertiary amine detected by NMR through an increasing of the ΔN8 value.

Pma–Pd complexes as catalytic systems for Suzuki–Miyaura reaction

Both data in solution and in the solid state indicate that the Pd–N bond length is deeply depending on the steric crowding at the pendant arm nitrogen atom. Chemical shifts observed and Δδ for protons, carbons, and nitrogen atoms calculated in the presence of additional electron donating groups are also consistent with an electronic enrichment of the N8 atom. These features are expected to impact catalytic activities of pma–Pd complexes within the Suzuki–Miyaura coupling context. We recently evidenced that pma-based catalysts could be used for the formation of carbon–carbon bonds through Suzuki–Miyaura reaction.[6,8] The evaluation of the catalytic efficiency and the role of substitution pattern at the pma core have been realized using 2-methoxy-1,1′-binaphthyl **11** as model compound. As shown below, the latter represents a convenient target as methoxy groups of the reactant **12** (4.05 ppm), the side product **14** (3.94 ppm), and the binaphthyl target **11** (3.77 ppm) could be clearly identified in ^{1}H NMR spectra of crude material (Scheme 2). The presence of the side product **14** plausibly arises from debromination of the starting material during catalytic process after the oxidative addition step. The latter process plausibly evolves concomitantly to the further transmetallation step, which is mandatory to the formation of the expected product **12**. Both competitive processes are worth to evaluate. Within this context, **11**/**12** and **11**/**14** ratios allow an easy and direct interpretation of both catalytic efficiency and selectivity respectively. Complex **5** could not be compared with all other complexes due to low solubility in the toluene/EtOH/H_2O solvent system used. Reactions were realized using 5% of catalytic system loading, 2 eq. of the boronic acid **13** and 4 eq of Cs_2CO_3 as the base in toluene/EtOH/H_2O: 1/1/0.5 as the solvent.

Complex **7** was first evaluated as the catalytic system for the obtention of binaphthyl derivative **11**. Disappointingly, **1**/**8** and **1**/**2** ratios of **11**/**12** and **11**/**14**, respectively, were observed after 3 h reaction course (Table 3, entry 1). If the **11**/**12** ratio remained unchanged after 13 h, a large increase of the amount of debromination the side product **14** was observed (entry 2). Moving from **7** to complex **8** bearing an additional methyl group revealed beneficial to the formation of **11** by comparison with **7**.

Table 3. Comparison of catalytic activity

Entry	Time (h)	Catalytic system	Ratio 11/12[a]	Ratio 11/14[b]
1	3	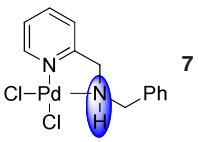 **7**	1/8	1/2
2	13		1/8	1/4.5
3	3	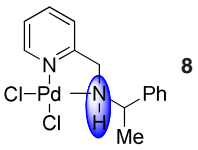 **8**	1/5	1/1.8
4	13		1/5	1/1.8
5[b]	24	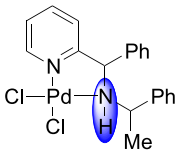	1/0	1/0.3
6	3	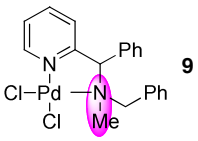 **9**	1/2	1/0.3
7	13		1/1	1/0.3
8	20		1/0.7	1/0.2
9	30		1/0.6	1/0.2
10	3	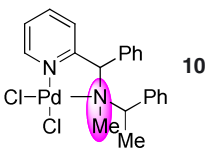 **10**	1/1.8	1/0.3
11	13		1/0.35	1/0.15
12	20		1/0.1	1/0.15
13	24		1/0.1	1/0.15

[a]Determined by ^{1}H NMR on the crude material.
[b]See the work by Grach *et al.*[8]

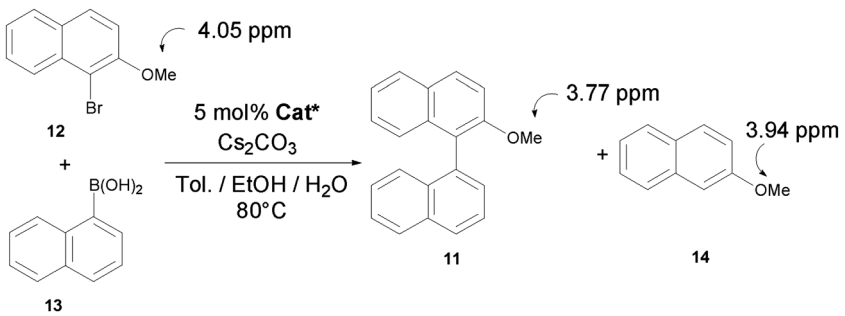

Scheme 2. Evaluation of the catalytic activity of pma-based Pd complexes.

However, initial **11**/**12** and **11**/**14** ratios did not evolve over a 13-h period (entries 3–4).

Interestingly, the joint presence of phenyl and methyl groups at both benzylic position and pendant arm nitrogen atom in the complex **9** allowed reaching higher efficiency and selectivity. Indeed, the formation of the target **11** gradually increased until it was the major product formed (entries 6–9).

In addition, the use of **9** also allowed limiting the formation of the side product **14** to a 1/0.2 ratio. A further increase of substitution as displayed in the complex **10** was finally examined. The use of **10** led to a clear improvement of catalytic efficiency (entries 10–13) showing a decrease of the starting bromide **12** until residual ratio of 1/0.1. Furthermore, the formation of **14** could also be limited to a 1/0.15 ratio, again largely favoring

the formation of the expected coupling product. The presence of a tertiary amine has thus a clear beneficial impact on the catalytic efficiency of pma-based series of palladium complexes shown in this study.

These results have however to be compared with previously reported data (entry 5) in which the *NH* analogue of **10** furnished a complete conversion and an **11**/**14** ratio of 1/0.3 within 24h reaction course. If a complete conversion using complex **10** could not be obtained in 24 h, our results suggest that **10** would generate lesser amount of the side product **14** being thus competitive as catalytic system. Our results allow confirming preliminary results and raising a general trend in the context of pma-based Pd complexes and Suzuki–Miyaura reaction. At first, a large substituent at the benzylic position was required for the obtention of fair to complete conversions. Second, the presence of a tertiary amine with all electron donor groups (Ph and Bn) induced a clear electronic enrichment of the pendant arm nitrogen atom in full agreement with liquid state NMR together with an increase of the steric crowding in accordance with solid state data and liquid NMR. Third, installation of additional substituents at pma-ligands revealed competitive in the context of catalytic efficiency and beneficial to selectivity by decreasing the formation of side products.

Conclusions

A complete analysis of a set of five pma ligands and their respective Pd complexes have been investigated. A full chemical shift study for ^{1}H, ^{13}C, and ^{15}N has been envisioned for ligands and complexes. ^{15}N chemical shifts coming from sensitive ^{15}N–^{1}H HMBC have been the most interesting data for feeling the design of the ligand on the strength of Pd–N bonds. NMR showed its potential to probe Pd surrounding at atomic resolution. This technique allows a clear identification of electronic distribution by comparing ligands to complexes chemical shifts at atomic resolution. The electronic contribution of each group on the pendant arm can be quantified by NMR. The most sensitive nuclei to detect the effect of the ligand design changes are constitutive of the metallacycle. The general trend is an increase of the $\Delta\delta$ for spectators ^{1}H, ^{13}C, and ^{15}N of the metallacycle because of the increase of the ligand electron density and especially on the pendant arm nitrogen atom. Moreover, the effect of the increasing steric hindrance by adding Ph, Me, and benzyl moieties tends on one hand to decrease the Pd–N bonds strength and on another hand to increase $\Delta\delta$. These results are in complete agreement with the X-ray data. Pma–Pd complexes have been successfully used as catalysts within the binaphthyl series. The comparison of five pma–Pd complexes showed that conversion and selectivity are strongly related to the substitution pattern at the pendant arm fitting with X-ray data. The presence of sterically hindered moieties (Ph, Me, and benzyl) has been showed beneficial to catalytic activity. Such substituents also account for an overall increase of electronic contribution of the ligand, which is in complete agreement with measured chemical shifts observed. Our study evidenced NMR as a pertinent and insightful tool to design ligands at atomic resolution in order to probe atoms of the ligand being the most involved in the reactivity of the Pd complexes.

Experimental Section

Experimental details for the preparation of the ligand **5** and the complex **10**, ^{1}H NMR, ^{13}C NMR spectra, and detailed NMR Tables 1, 2, 3, and 4 are given in the Supporting Information.

Acknowledgements

The authors are grateful to the CNRS, the Universities of Paris Sud and Versailles-St Quentin-en-Yvelines, ANR (ANR-11-BS07-030-01). This work is supported by a public grant overseen by the French National Research Agency (ANR) as part of the «Investissements d'Avenir » program n° ANR -11- IDEX-0003-02 and CHARMMMAT ANR - 11-LABEX-0039.

References

[1] a)K. Suzuki, P. D. Oldenburg, L. Que Jr. *Angew. Chem. Int. Ed.* **2008**, 47, 1887–1889; b)C. Hemmert, M. Renz, H. Gornitzka, B. Meunier. *J. Chem. Soc. Dalton Trans.* **1999**, 3989–2994. c)C. Hemmert, M. Renz, H. Gornitzka, S. Soulet, B. Meunier. *Chem. Eur. J.* **1999**, *5*, 1766–1774. d)M. Wu, B. Wang, S. Wang, C. Xia, W. Sun. *Org. Lett.* **2009**, *11*, 3622–3625. e)D. V. Griffiths, M. J. Al-Jeboori, P. J. Arnold, Y.-K. Cheong, P. Duncanson, M. Motevalli. *Inorg. Chim. Acta* **2010**, 363, 1186–1194; f)P. J. Arnold, S. C. Davies, M. C. Durrant, D. V. Griffiths, D. L. Hughes, P. C. Sharpe. *Inorg. Chim. Acta* **2003**, 348, 143–149; g)S. Zhu, W. W. Brennessel, R. G. Harrison, L. Jr. Que, *Inorg. Chim. Acta* **2002**, *337*, 32–38. h)J. M. Rowland, M. M. Olmstead, P. K. Mascharak. *Inorg. Chem.* **2000**, *39*, 5326–5332. i)Y.-H. Chiu, O. dos Santos, J. W. Canary. *Tetrahedron* **1999**, *55*, 12069–12078. j)J. W. Canary, C. S. Allen, J. M. Castagnetto, Y.-H. Chiu, P. J. Toscano, Y. Wang. *Inorg. Chem.* **1998**, *37*, 6255–6262.

[2] a)J. M. Darmon, S. C. E. Stieber, K. T. Sylvester, I. Fernandez, E. Lobkovsky, S. P. Semproni, E. Bill, K. Wieghardt, S. DeBeer, P. J. Chirik. *J. Am. Chem. Soc.* **2012**, *134*, 17125–17137. b)W. N. Oloo, A. J. Fielding, L. Que Jr.. *J. Am. Chem. Soc.* **2013**, *135*, 6438–6441. c)C. J. Allpress, K. Grubel, E. Szajna-Fuller, A. M. Arif, L. M. Berreau. *J. Am. Chem. Soc.* **2013**, *135*, 659–668. d)J. Park, Y. Morimoto, Y.-M. Lee, W. Nam, S. Fukuzumi. *J. Am. Chem. Soc.* **2011**, *133*, 5236–5239. e)S. Hong, Y.-M. Lee, W. Shin, S. Fukuzumi, W. Nam. *J. Am. Chem. Soc.* **2009**, *131*, 13910–13911. f)O. Y. Lyakin, K. P. Bryliakov, G. J. P. Britovsek, E. P. Talsi. *J. Am. Chem. Soc.* **2009**, *131*, 10798–10799.

[3] M. W. Bouwkamp, A. C. Bowman, E. Lobkovsky, P. J. Chirik. *J. Am. Chem. Soc.* **2006**, *128*, 13340–13341.

[4] a)G. Blay, V. Hernandez-Olmos, J. R. Pedro. *Org. Lett.* **2010**, *12*, 3058–3061. b)G. Blay, V. Hernandez-Olmos, J. R. Pedro. *Chem. Commun.* **2008**, 4840–4842. c)G. Blay, L. R. Domingo, V. Hernandez-Olmos, J. R. Pedro. *Chem. Eur. J.* **2008**, *14*, 4725–4730.

[5] S. Marque, V. Razafimahaléo, A. Dinut, G. Grach, D. Prim, X. Moreau, R. Gil. *New J. Chem.* **2013**, 37, 2683–2690.

[6] V. Terrasson, D. Prim, J. Marrot. *Eur. J. Inorg. Chem* **2008**, 2739–2745.

[7] G. Grach, A.Dinut, S. Marque, J. Marrot, R. Gil, D. Prim. *Org. Biomol. Chem.* **2011**, *9*, 497–503.

[8] G. Grach, G. Pieters, A. Dinut, V. Terrasson, R. Medimagh, A. Bridoux, V. Razafimahaleo, A. Gaucher, S. Marque, J. Marrot, D. Prim, R. Gil, J. Giner Planas, C. Vinas, I. Thomas, J.-P. Roblin, Y. Troin. *Organometallics* **2011**, *30*, 4074–4086.

[9] V. Terrasson, S. Marque, A. Scarpacci, D. Prim. *Synthesis* **2006**, *11*, 1858–1862.

[10] B. Puget, J.-P. Roblin, D. Prim, Y. Troin. *Tetrahedron Lett.* **2008**, *49*, 1706–1709.

[11] V. Terrasson, J. Giner Planas, C. Vinas, F. Teixidor, D. Prim, M. E. Light, M. B. Hursthouse. *Organometallics* **2010**, *29*, 4130–4134.

[12] a)D. Niedzielska, T. Pawlak, T. Czubachowski, L. Pazderski. *J. Spect.* **2013**, *2013*, 1–8. b)L. Pazderski. *Magn. Reson. Chem.* **2008**, *46*, S3.

[13] a)A. Bax, M. F. Summers. *J. Am. Chem. Soc.* **1986**, *108*, 2093–2094. b)E. Szłyk, L. Pazderski, I. Łakomska, L. Kozerski, J. Sitkowski. *Magn. Reson. Chem.* **2002**, *40*, 529–532.

[14] CCDC 677262 see ref 6/ CCDC 677264 see ref 6/ CCDC 812300 see ref 8/ CCDC 812301 see ref 8/ CCDC 812302 see ref 8.

Supporting Information

Additional supporting information may be found in the online version of this article at the publisher's website.